Macromolecules

Article

pubs.acs.org/Macromolecules

Electrostatic Effects on the Conformation and Elasticity of Hyaluronic Acid, a Moderately Flexible Polyelectrolyte

John P. Berezney[†] and Omar A. Saleh*[,†,‡]

[†]Materials Department and [‡]BMSE Program, University of California, Santa Barbara, Santa Barbara, California 93106, United States

Supporting Information

ABSTRACT: Hyaluronic acid (HA) is a charged polysaccharide with an intrinsic stiffness intermediate between flexible and semiflexible polymers. To investigate the interplay of that stiffness with solution electrostatic interactions, we perform single-molecule stretching measurements on HA over 4 decades of monovalent ionic strength. We observe a low-force (<1 pN), salt-sensitive swollen (Pincus) elasticity regime and use a rescaling analysis to show that the data are inconsistent with a quadratic, "OSF" dependence of the chain's persistence length on the solution Debye length. Instead, the persistence length varies nearly linearly with Debye length. The chain's high-force (1−10 pN) elastic response deviates from exact worm-like chain models, even after accounting for electrostatic effects; the failure of these models emphasizes the utility of both low-force data and a robust scaling-based analysis scheme. Our results give insight into electrostatic effects in an intermediately stiff polymer as well as demonstrating elastic phenomena that could impact understanding of HA's mechanobiological roles.

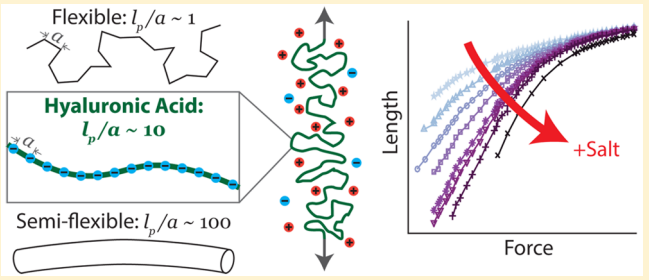

INTRODUCTION

Charged polymers, or polyelectrolytes, are stiffened by electrostatic repulsion between their monomers. In turn, mobile salt ions in the solution screen the repulsion, leading to a salt-dependent chain stiffness for polyelectrolytes. This effect is of particular importance in defining the physical behavior of biolological macromolecules, since they are typically highly charged and since biological solutions are characterized by considerable concentrations of salt.

The electrostatic stiffening effect, and its dependence on salt, has been the subject of intense discussion. Following Odijk[1] and Skolnick and Fixman,[2] the effect is typically parametrized by separating the local stiffness into an intrinsic persistence length, l_p^0, arising from nonelectrostatic interactions (bond stiffnesses and rotational freedoms, steric interactions, etc.), and an electrostatic persistence length, l_e, highly sensitive to salt concentration. Multiple theoretical models make predictions (not always in agreement) on the behavior of l_e with salt, typically in the limit of either relatively stiff, "semiflexible" chains (with $l_p^0 \gg a$ where a is the length of the chemical repeat unit) or flexible chains (with $l_p^0 \approx a$). Experiments have focused on these same limits, frequently using double-stranded DNA (dsDNA) as a model semiflexible chain ($l_p^0/a \approx 150$)[3] and single-stranded nucleic acids (ssNAs) as model flexible chains ($l_p^0/a \approx 1$).[4,5] However, the electrostatic stiffening effect has not been extensively explored for chains of intermediate stiffness, $l_p^0/a \approx 10$.

Here, we undertake an experimental study of the electrostatic effects on the stiffness and conformational freedom of a model chain of intermediate stiffness: hyaluronic acid (HA). HA is a polysaccharide found in both eukaryotes and prokaryotes; in humans, it notably plays key roles in defining the behavior of extracellular spaces.[6−8] HA has further found wide practical use in biotechnology as a scaffold for cell growth and drug delivery.[9−12] Structurally, HA is a linear polymer composed of D-glucuronic acid and D-*N*-acetylglucosamine dimers. On long length scales, HA forms a self-avoiding random coil due to its solubility in water and associated lack of higher order (folded) structure.[13] On shorter length scales, HA is stiffened by monomer−monomer interactions, including dynamic hydrogen bonding, water bridging, and the electrostatic repulsion between the glucuronic acid carboxyl groups along the highly charged (1 e/nm) backbone.[14] These interactions lead to an intrinsic persistence length ($l_p^0 \approx 5$ to 10 nm[15]) somewhat larger than the size of the disaccharide repeat unit ($a \approx 1$ nm). Thus, HA is a biopolymer of intermediate rigidity: $l_p^0/a \approx 5-10$, which is 10-fold more flexible than dsDNA, yet 10-fold stiffer than ssNAs.

We investigate HA's mechanics using single-molecule stretching experiments. We observe distinct low- and high-force elastic regimes and analyze the salt dependence of those regimes to probe electrostatic stiffening of the chain. Our study derives new insight from the ability to access the low-force regime and its associated self-avoiding random-walk conformations. This is enabled because, in contrast to prior stretching

Received: October 4, 2016
Revised: January 10, 2017

DOI: 10.1021/acs.macromol.6b02166
Macromolecules XXXX, XXX, XXX−XXX

studies of HA,[16] we utilize an experimental technique (the magnetic tweezers) capable of stable application of small forces.

EXPERIMENTAL SECTION

High molecular weight HA (2.5 MDa, ≈6000 repeat units, contour length ≈6000 nm) was purchased from Creative PEGworks with a single biotin group incorporated at the reducing end, and thiol groups incorporated randomly within the chain with a stoichiometry of one thiol per chain. The thiol groups were attached to maleimide-functionalized, PEG-grafted glass surfaces (Microsurfaces, Inc.) in solutions of 10 nM HA, 100 mM TCEP, 50 mM sodium phosphate buffer (pH 7.2), and 50 mM NaCl. This was rinsed with a solution of 1 mM MOPS buffer (pH 7.5) and 0.001% Tween-20. The biotin ends of the molecules were bound to 1 μm diameter, streptavidin-coated paramagnetic beads (Invitrogen). These beads were added to the flow cell and incubated 10 min; unbound beads were then rinsed away.

The flow cell containing bead/HA tethers was then placed into a custom-built magnetic tweezer instrument[17] for single-molecule elastic testing. Briefly, the instrument uses a stepper motor to bring a magnetic assembly in near proximity to the flow cell, generating an adjustable magnetic field gradient that pulls on the beads, stretching attached chains. Chain extension is measured through optical tracking of the height of the bead. The tension is measured individually for each bead by measuring that bead's lateral thermal fluctuations and applying a Langevin analysis that models the system as a pendulum undergoing overdamped Brownian motion.[18]

Experiments were conducted with magnetic tweezers in 0.1−1 mM MOPS buffer (pH 7.5), 0−5000 mM NaCl, and 0.001% Tween-20. The total ionic strength, I, of the solution is the sum of the NaCl concentration and 40% of the MOPS concentration (which accounts for the partial protonation of the buffering agent). At low pH (<4), the HA charge density is dependent on the ionic strength of the solution;[19] this complication is avoided here by performing our experiments at higher pH.

The stochastic labeling method leads to polydispersity in the length of HA tethers; thus, comparing force−extension data from different molecules could create systematic errors. To avoid this, we acquire a set of force−extension curves over a range of salt concentrations on each individual molecule (always including a reference curve at I_{ref} = 1.4 mM) and compute salt dependencies relative to the reference curve.

REGIMES OF HA ELASTIC RESPONSE

The extension of HA tethers increases smoothly and continuously with the application of force (Figure 1A), consistent with a lack of folded structures. We conceptualize the elastic response by considering the tensile screening length, $\xi = k_BT/f$, which represents the length scale beyond which polymer looping driven by thermal energy, k_BT, is suppressed by the applied force, f.[20] The effects of long-range interactions are thus present at low forces but not at high forces. Correspondingly, in the force−extension data, two distinct regimes of elastic response are apparent: at low forces, the polymer extends as a nonlinear power law of the force while, at higher forces, the polymer displays a less compliant elastic behavior that approaches lengths approximately equal to the expected tethered lengths of the molecules.

The low-force elasticity follows a power law with an exponent of about 2/3, though this shows some dependence on the ionic strength: At 500 mM, the exponent exceeds 2/3 and approaches 1, while at low salt concentrations the exponent is slightly below 2/3 (Figure 1B, inset). The presence of the 2/3 value is characteristic of the Pincus blob scaling regime which describes the elasticity of a chain of tensile blobs of size ξ swollen by excluded volume interactions,[20] while an exponent of 1 is instead expected for an ideal chain. Thus, the salt

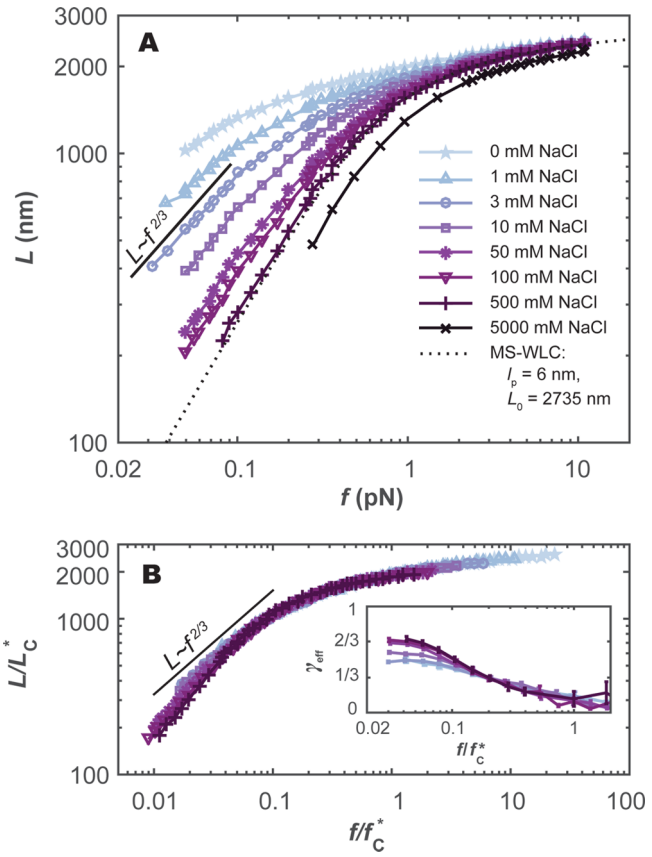

Figure 1. (A) Representative data of extension versus applied force collected from a single hyaluronic acid molecule at various salt concentrations. The data at 500 mM NaCl are fit to a worm-like chain model with a best-fit contour length of 2735 nm and persistence length of 5.9 nm (dotted line). (B) Master curve found from rescaling each force extension curve from (A) by the salt-dependent parameters f_c^* and L_c^*. The 5 M NaCl data are omitted. Inset: the force dependence of the local power law exponent γ, found by analyzing polymer fluctuations. The data shown is an average over seven molecules. Low-force values of γ approach the Pincus exponent of 2/3.

dependence of the exponent can be understood as a good-to-theta solvent transition as the salt concentration increases. A similar effect was seen in the elasticity of single-stranded DNA,[5] though in that case the exponent held constant near 2/3 over a broad range of salt, before transitioning relatively suddenly to the theta value of 1 at high salt. In contrast, our measurements of HA indicate a broad "marginal" solvent regime, with the exponent slowly increasing with salt, indicative of elastic behavior falling between that expected in the good and theta limits.

To carefully examine the low-force elasticity, we estimate the power-law exponent of the force−extension curve from measured fluctuations using a parameter called the effective exponent, γ_{eff} (Figure 1B, inset).[21,22] This analysis does not depend on the absolute tether length and so provides an estimate independent of that found from direct fitting of force−extension curves. The fluctuations in the direction of extension can be related to the slope of the elastic curve through the fluctuation−dissipation relation.[21,22] By assuming a power-law elastic relation, the local power-law exponent is estimated from the ratio of fluctuations of the polymer end in the directions orthogonal and parallel to the pulling direction; we measure this through tracking the trajectory of the tethered bead over

DOI: 10.1021/acs.macromol.6b02166
Macromolecules XXXX, XXX, XXX−XXX

time at constant force. This data reaffirms the broad marginal-solvent behavior seen in the force–extension curves: at low salt, the effective exponent plateaus near 2/3 at low force; at higher salt, this plateau value slowly increases.

ELASTIC REGIME CROSSOVER PERMITS QUANTIFICATION OF SALT-DEPENDENT HA STIFFNESS

The Pincus elastic regime is expected to persist until ξ becomes comparable to the statistical monomer size (Kuhn length), which depends on l_p.[5,23] Thus, the elastic regime crossover can be used to estimate microscopic structural parameters of the chain. Particularly, if we assume the Pincus regime to end at a crossover force $f_c \sim k_BT/l_p$, then the full Pincus elastic expression gives the scaling of the inter-regime crossover extension, L_c, as $L_c \sim L_0(\nu/l_p)^{1/3}(f_c/k_BT)^{2/3} \sim L_0(\nu/l_p^3)^{1/3}$, where L_0 is the contour length and ν is the excluded volume parameter.[5] The elastic response in both regimes is controlled by the microscopic parameters l_p and ν, which determine the values of the crossover parameters; thus, by rescaling the elastic curves by the crossover values, we expect to observe universal elastic behavior. In our experimental analysis, we invert this dependence: we find rescaling parameters, f_c^* and L_c^*, that collapse all curves (Figure 1B) by fitting each curve onto the 1.4 mM data.[24] We then assert that the rescaling parameters thus extracted are proportional to the crossover force and length, and so can be used to understand the salt-dependent properties of the structural parameters, l_p and ν. The data on L_c^* show only a very weak dependence on I (see Supporting Information), indicative of a chain with $\nu \sim l_p^3$. For a rod-like chain, the expectation is $\nu \sim l_p^2 d$, where d is the chain diameter; thus, our data are consistent with statistical chain segments whose length and diameter are similar, presumably because both are dominated by electrostatic interactions. That said, our primary focus in this work is on the behavior of f_c^*, which reports on l_p.

At low ionic strength, the values for f_c^* increase roughly as the square root of the ionic strength: direct fitting of a power law to the $I \leq 10.4$ mM data gives $f_{c,PL}^* \propto I^{0.55\pm0.01}$ (Table 1 and Figure 2). As the salt concentration is increased, f_c^* plateaus (Figure 2). For polyelectrolytes, it is conventional to consider the persistence length as the sum of a salt-independent intrinsic persistence length and a salt-dependent electrostatic persistence length, $l_p = l_p^0 + l_e(I)$. The screening effect of high ionic strength solvent environments will decrease l_e toward zero, causing the intrinsic value to dominate; this effect explains the plateau in f_c^* for $I > 50$ mM. At about 50 mM, the Debye length of the solution decreases below the charge spacing along the HA backbone, so a reduction of electrostatic effects is expected.

Table 1. Summary of Extracted Values from Fits to Models Describing the Dependence of f_c^* on Ionic Strength[a]

model	N	k	χ_{red}^2	α	I_c (mM)
$f_{c,BJ}^*$	8	1	17	0.5	167 ± 26
$f_{c,OSF}^*$	8	1	37	1	4.4 ± 0.2
$f_{c,free}^*$	8	2	2.4	0.65 ± 0.02	21 ± 4
$f_{c,PL}^*$	5	1	2.4	0.55 ± 0.01	N/A

[a] N indicates the number of data points used in the fitting, and k indicates the number of free parameters in the model.

To analyze the crossover behavior of f_c^*, we fit the data to a model that accounts both for the expected additivity of intrinsic and electrostatic persistence lengths (i.e., enforcing $f_c^* \propto k_BT/(l_p^0 + l_e(I))$ and for the rescaling procedure by enforcing $f_c^* = 1$ at $I_{ref} = 1.4$ mM). In particular, we fit to

$$f_c^*(I) = \frac{1 + (I_c/I_{ref})^\alpha}{1 + (I_c/I)^\alpha} \quad (1)$$

where I_c defines the ionic strength beyond which f_c^* plateaus and α is an exponent controlling the power-law dependence of the electrostatic persistence length on I, $l_e(I) \sim I^{-\alpha}$; best-fit parameters are described in Table 1. We first carry out one-parameter fits, allowing I_c to vary, while fixing $\alpha = 0.5$ or $\alpha = 1$. The former, termed $f_{c,BJ}^*$, enforces a linear dependence of l_e on solution Debye length, as predicted by a host of theoretical models including Barrat–Joanny (BJ).[25−28] The $f_{c,OSF}^*$ model fixes $\alpha = 1$, enforcing a quadratic dependence on Debye length, as predicted by the Odijk–Skolnick–Fixman (OSF) model.[1,2] The BJ fit clearly outperforms the OSF fit, though neither is a statistically perfect descriptor, as judged by the reduced χ^2, χ_{red}^2, goodness-of-fit metric (see Table 1). [Note that $\chi_{red}^2 \approx 1$ is expected for a model that correctly fits (but does not overfit) a set of noisy data, while $\chi_{red}^2 \gg 1$ indicates a poor fit.] A statistically good fit is obtained using the $f_{c,free}^*$ model, in which eq 1 is fit with two free parameters, I_c and α (Table 1). The best-fit result, $\alpha = 0.65 \pm 0.02$, still suggests a change in persistence length with added salt that deviates significantly from the OSF picture.

Previous experimental results indicate that OSF behavior is not followed by flexible polyelectrolytes.[4,5,29,30] Certain prior results argue that OSF behavior is seen in stiff polyelectrolytes such as dsDNA,[3] but this is questioned by more recent work.[31] Experiments specific to HA are also divided.[32,33] Our results, on a polymer of intermediate stiffness, cast further doubt on the range of applicability of the OSF prediction.

The failure of the OSF prediction could be due to OSF's underlying assumption of linear, Debye–Hückel, solution electrostatics. It has been shown that nonlinear solution electrostatic effects can lead to a variation of the chain's effective charge density with salt; this manifests as a reduced sensitivity of the persistence length to ionic strength relative to the OSF model.[34] Intriguingly, this nonlinear theory predicts $l_p \sim I^{0.7}$, consistent with the exponent of 0.65 ± 0.02 found here.

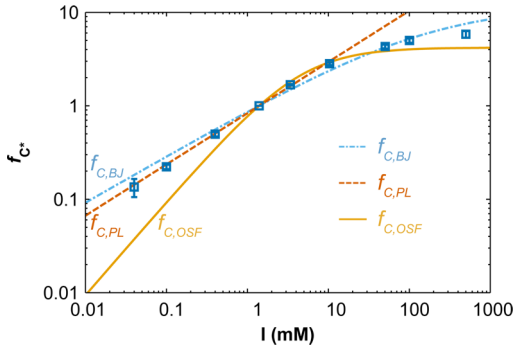

Figure 2. Dependence of the rescaling parameters, f_c^*, on ionic strength; error bars indicate the standard error of the mean. The data are fit to eq 1, with electrostatic persistence length assumed to follow Barrat–Joanny (BJ) or Odijk–Skolnick–Fixman (OSF) behavior. Also shown is a fit to a power law, $f_c^* \sim I^\alpha$, to the low-salt ($I \leq 10.4$ mM) data, with best-fit exponent noted. Data are collected from 12 separate molecules.

DOI: 10.1021/acs.macromol.6b02166
Macromolecules XXXX, XXX, XXX–XXX

ANALYSIS OF HIGH-FORCE HA ELASTICITY

In the high-force regime, the lack of swelling interactions permits analysis of the data using exact elastic models, rather than scaling approaches. In the highly stretched regime, the conformation is that of a straight chain with slight bending perturbations orthogonal to the axis of tension. For a neutral chain in this regime, the Marko−Siggia worm-like chain model is expected to hold.[35] We account for electrostatic interactions in an ad hoc manner by inserting a BJ-like term (linear in Debye length) into the Marko−Siggia expression, giving a model we term the MS-BJ:

$$L/L_0 = 1 - \sqrt{\frac{k_B T}{4(l_p^0 + \beta I^{-0.5})f}} \quad (2)$$

where β is a fitting parameter. A more refined approach, carried out by Marko and Siggia,[35] accounts for electrostatics by explicitly modeling the effect of the chain's charge spacing, b, on the electrostatic energy of the bending modes.[27,35] This approach, here termed MS-Modes, has been applied to stiff dsDNA[35] and enforces an OSF-like electrostatic persistence length. Thus, the MS-BJ model is more internally consistent with the findings of non-OSF behavior from the rescaling analysis (Figure 2).

We analyze the high-force elasticity regime by performing one-parameter fits of the two models to data with $L > L_0/2$ across all salt concentrations. The fitted parameter is either a scaling parameter, β (for MS-BJ), or the linear charge spacing, b (for MS-Modes). The other parameters, L_0 and l_p^0, are fixed to the values extracted from an MS-WLC fit to the data at I = 500 mM. Both fits capture aspects of the behavior, but neither accurately describes the full salt dependence. As seen in Figure 3, the MS-BJ fit captures the salt dependence for $I \lesssim 500$ mM but does increasingly worse at lower salt. Conversely, the MS-modes fit performs best at the lowest salt and worse close to 500 mM. In quantitative terms, and reporting values as (mean ± standard error) across five molecules, the MS-BJ fit returns β = 6.3 ± 0.6 and a goodness-of-fit metric χ_{red}^2 = 32 ± 5, while MS-Modes returns b = 0.77 ± 0.03 nm and χ_{red}^2 = 67 ± 33. Thus, neither fit is a statistically good descriptor of the data, though it is encouraging that the best-fit charge spacing from MS-Modes is similar to the structural value of 1 nm.

The two fitted models enforce different electrostatic behaviors; yet, our data are unable to differentiate them. This is likely because a chain's high-force elastic response is not a sensitive indicator of it is electrostatic behavior, since the electrostatic effects on conformation are minimal for a chain that is already straightened by force. If correct, this interpretation calls into question prior conclusions on the OSF-like behavior of dsDNA based on high-force elastic measurements.[3,35] Alternatively, the poor fit quality could be because the models themselves are faulty, either due to incorrect assumptions (such as the Debye−Hückel approximation of solution electrostatics that underlies MS-Modes) or due to missing physical effects. Such missing effects could include force-induced structural transitions in HA, as are known to occur in other carbohydrates,[36] or remnant effects of swelling on the high-force elasticity, as was recently observed in simulations.[37]

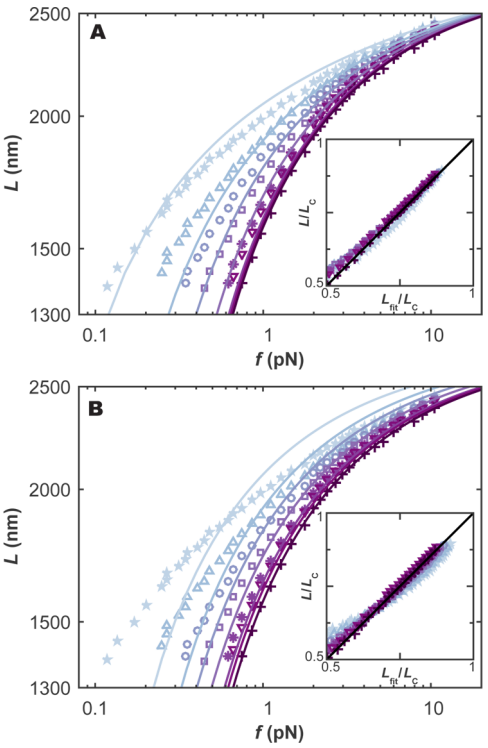

Figure 3. Force−extension data from Figure 1 are globally fit, solely at high extensions ($0.5L_0 < L < L_0$), in (A) to the MS-Modes expression and in (B) to the MS-BJ relation (eq 2) as described in the text. For the fit shown, Insets: normalized extension against fitted extension for the two fits, showing salt-dependent deviations from the models. Legend is the same as Figure 1.

CONCLUSIONS

We have shown through direct single-molecule measurements that hyaluronic acid exhibits salt-dependent swollen-chain elasticity. Our rescaling analysis of the entire elastic curve is firmly inconsistent with the standard OSF electrostatic-stiffening model, joining a growing body of work on various polymers that questions the applicability of that model. That same analysis is more consistent with an electrostatic persistence length that varies with ionic strength as $I^{-0.5}$ (that is, linearly with solution Debye length) in the low-salt regime: across all fitting methods tested, the most sensitive dependence found was $I^{-0.65}$. We further show the high-force elastic behavior has clear deviations from exact elastic predictions that include electrostatic effects. This indicates the difficulty in interpreting electrostatic behavior solely from high-force elasticity measurements, thus emphasizing both the utility of elastic data measured over a wide range of forces and the relative power of our rescaling analysis.

ASSOCIATED CONTENT

Supporting Information

The Supporting Information is available free of charge on the ACS Publications website at DOI: 10.1021/acs.macromol.6b02166.

Figure S1 (PDF)

DOI: 10.1021/acs.macromol.6b02166
Macromolecules XXXX, XXX, XXX−XXX

AUTHOR INFORMATION

Corresponding Author

*E-mail: saleh@engineering.ucsb.edu; Ph +1 805 8938814; Fax +1 805 8938486 (O.A.S.).

ORCID

Omar A. Saleh: 0000-0002-9197-4024

Notes

The authors declare no competing financial interest.

ACKNOWLEDGMENTS

This work was supported by the NSF under Grants DMR-1309414 and DMR-1611497. The authors thank P. Pincus and P. A. Janmey for helpful conversations.

REFERENCES

(1) Odijk, T. Polyelectrolytes near the Rod Limit. *J. Polym. Sci., Polym. Phys. Ed.* **1977**, *15*, 477−483.

(2) Skolnick, J.; Fixman, M. Electrostatic Persistence Length of a Wormlike Polyelectrolyte. *Macromolecules* **1977**, *10*, 944−948.

(3) Baumann, C. G.; Smith, S. B.; Bloomfield, V. A.; Bustamante, C. Ionic effects on the elasticity of single DNA molecules. *Proc. Natl. Acad. Sci. U. S. A.* **1997**, *94*, 6185−6190.

(4) Jacobson, D. R.; McIntosh, D. B.; Saleh, O. A. The Snakelike Chain Character of Unstructured RNA. *Biophys. J.* **2013**, *105*, 2569−2576.

(5) Saleh, O. A.; McIntosh, D. B.; Pincus, P.; Ribeck, N. Nonlinear Low-Force Elasticity of Single-Stranded DNA Molecules. *Phys. Rev. Lett.* **2009**, *102*, 068301.

(6) Toole, B. P. Hyaluronan: from extracellular glue to pericellular cue. *Nat. Rev. Cancer* **2004**, *4*, 528−539.

(7) Lokeshwar, V. B.; Selzer, M. G. Differences in hyaluronic acid-mediated functions and signaling in arterial, microvessel, and vein-derived human endothelial cells. *J. Biol. Chem.* **2000**, *275*, 27641−27649.

(8) Laurent, T. C.; Fraser, J. R. E. Hyaluronan. *FASEB J.* **1992**, *6*, 2397−2404.

(9) Collins, M. N.; Birkinshaw, C. Hyaluronic acid based scaffolds for tissue engineering-A review. *Carbohydr. Polym.* **2013**, *92*, 1262−1279.

(10) Kogan, G.; Soltes, L.; Stern, R.; Gemeiner, P. Hyaluronic acid: a natural biopolymer with a broad range of biomedical and industrial applications. *Biotechnol. Lett.* **2006**, *29*, 17−25.

(11) Leach, J. B.; Bivens, K. A.; Patrick, C. W.; Schmidt, C. E. Photocrosslinked hyaluronic acid hydrogels: Natural, biodegradable tissue engineering scaffolds. *Biotechnol. Bioeng.* **2003**, *82*, 578−589.

(12) Luo, Y.; Kirker, K. R.; Prestwich, G. D. Cross-linked hyaluronic acid hydrogel films: new biomaterials for drug delivery. *J. Controlled Release* **2000**, *69*, 169−184.

(13) Laurent, T. C.; Laurent, U. B.; Fraser, J. R. Functions of hyaluronan. *Ann. Rheum. Dis.* **1995**, *54*, 429−432.

(14) Almond, A.; Brass, A.; Sheehan, J. K. Oligosaccharides as Model Systems for Understanding Water-Biopolymer Interaction: Hydrated Dynamics of a Hyaluronan Decamer. *J. Phys. Chem. B* **2000**, *104*, 5634−5640.

(15) Fouissac, E.; Milas, M.; Rinaudo, M.; Borsali, R. Influence of the ionic strength on the dimensions of sodium hyaluronate. *Macromolecules* **1992**, *25*, 5613−5617.

(16) Giannotti, M. I.; Rinaudo, M.; Vancso, G. J. Force Spectroscopy of Hyaluronan by Atomic Force Microscopy: From Hydrogen-Bonded Networks toward Single-Chain Behavior. *Biomacromolecules* **2007**, *8*, 2648−2652.

(17) Ribeck, N.; Saleh, O. A. Multiplexed single-molecule measurements with magnetic tweezers. *Rev. Sci. Instrum.* **2008**, *79*, 094301−6.

(18) Lansdorp, B. M.; Saleh, O. A. Power spectrum and Allan variance methods for calibrating single-molecule video-tracking instruments. *Rev. Sci. Instrum.* **2012**, *83*, 025115−10.

(19) Cleland, R. L.; Wang, J. L.; Detweiler, D. M. Polyelectrolyte properties of sodium hyaluronate. 2. Potentiometric titration of hyaluronic acid. *Macromolecules* **1982**, *15*, 386−395.

(20) Pincus, P. Excluded Volume Effects and Stretched Polymer Chains. *Macromolecules* **1976**, *9*, 386−388.

(21) Saleh, O. A. Perspective: Single polymer mechanics across the force regimes. *J. Chem. Phys.* **2015**, *142*, 194902.

(22) McIntosh, D. B.; Duggan, G.; Gouil, Q.; Saleh, O. A. Sequence-Dependent Elasticity and Electrostatics of Single-Stranded DNA: Signatures of Base-Stacking. *Biophys. J.* **2014**, *106*, 659−666.

(23) Netz, R. R. Strongly Stretched Semiflexible Extensible Polyelectrolytes and DNA. *Macromolecules* **2001**, *34*, 7522−7529.

(24) McIntosh, D. B.; Saleh, O. A. Salt Species-Dependent Electrostatic Effects on ssDNA Elasticity. *Macromolecules* **2011**, *44*, 2328−2333.

(25) Dobrynin, A. V.; Carrillo, J.-M. Y. Swelling of biological and semiflexible polyelectrolytes. *J. Phys.: Condens. Matter* **2009**, *21*, 424112.

(26) Ha, B. Y.; Thirumalai, D. Electrostatic Persistence Length of a Polyelectrolyte Chain. *Macromolecules* **1995**, *28*, 577−581.

(27) Barrat, J. L.; Joanny, J. F. Persistence Length of Polyelectrolyte Chains. *Europhys. Lett.* **1993**, *24*, 333−338.

(28) Ullner, M.; Jönsson, B.; Peterson, C.; Sommelius, O.; Söderberg, B. The electrostatic persistence length calculated from Monte Carlo, variational and perturbation methods. *J. Chem. Phys.* **1997**, *107*, 1279−1287.

(29) Nishida, K.; Urakawa, H.; Kaji, K.; Gabrys, B.; Higgins, J. S. Electrostatic persistence length of NaPSS polyelectrolytes determined by a zero average contrast SANS technique. *Polymer* **1997**, *38*, 6083−6085.

(30) Spiteri, M. N.; Boué, F.; Lapp, A.; Cotton, J. P. Persistence Length for a PSSNa Polyion in Semidilute Solution as a Function of the Ionic Strength. *Phys. Rev. Lett.* **1996**, *77*, 5218−5220.

(31) Brunet, A.; Tardin, C.; Salomé, L.; Rousseau, P.; Destainville, N.; Manghi, M. Dependence of DNA Persistence Length on Ionic Strength of Solutions with Monovalent and Divalent Salts: A Joint Theory-Experiment Study. *Macromolecules* **2015**, *48*, 3641−3652.

(32) Vuletić, T.; Dolanski Babić, S.; Ivek, T.; Grgičin, D.; Tomić, S.; Podgornik, R. Structure and dynamics of hyaluronic acid semidilute solutions: A dielectric spectroscopy study. *Phys. Rev. E* **2010**, *82*, 011922.

(33) Buhler, E.; Boué, F. Chain Persistence Length and Structure in Hyaluronan Solutions: Ionic Strength Dependence for a Model Semirigid Polyelectrolyte. *Macromolecules* **2004**, *37*, 1600−1610.

(34) Netz, R. R.; Orland, H. Variational charge renormalization in charged systems. *Eur. Phys. J. E: Soft Matter Biol. Phys.* **2003**, *11*, 301−311.

(35) Marko, J. F.; Siggia, E. D. Stretching DNA. *Macromolecules* **1995**, *28*, 8759−8770.

(36) Marszalek, P. E.; Oberhauser, A. F.; Pang, Y.-P.; Fernandez, J. M. Polysaccharide elasticity governed by chair-boat transitions of the glucopyranose ring. *Nature* **1998**, *396*, 661−664.

(37) Stevens, M. J.; Saleh, O. A. Simulations of stretching a flexible polyelectrolyte with varying charge separation. *Eur. Phys. J.: Spec. Top.* **2016**, *225*, 1683−1692.

DOI: 10.1021/acs.macromol.6b02166
Macromolecules XXXX, XXX, XXX−XXX